



1 Experimental observation of transient $\delta^{18}\text{O}$ interaction between snow and
2 advective airflow under various temperature gradient conditions

3

4 Pirmin Philipp Ebner¹, Hans Christian Steen-Larsen^{2,3}, Barbara Stenni^{4,5}, Martin
5 Schneebeli^{1,*}, and Aldo Steinfeld⁶

6 ¹ *WSL Institute for Snow and Avalanche Research SLF, 7260 Davos Dorf, Switzerland*

7 ² *LSCE Laboratoire des Sciences du Climat et de l'Environnement, Gif-Sur-Yvette Cedex, France*

8 ³ *Center for Ice and Climate, Niels Bohr Institute, University of Copenhagen, Copenhagen, Denmark*

9 ⁴ *Department of Environmental Sciences, Informatics and Statistics, University Ca' Foscari of Venice,
10 Venice, Italy*

11 ⁵ *Institute for the Dynamics of Environmental Processes, CNR, Venice, Italy*

12 ⁶ *Department of Mechanical and Process Engineering, ETH Zurich, 8092 Zurich, Switzerland*

13

14 **Abstract**

15 Stable water isotopes ($\delta^{18}\text{O}$) obtained from snow and ice samples of polar regions
16 are used to reconstruct past climate variability, but heat and mass transport processes
17 can affect the isotopic composition. Here we present an experimental study on the effect
18 on the snow isotopic composition by airflow through a snow pack in controlled
19 laboratory conditions. The influence of isothermal and controlled temperature gradient
20 conditions on the $\delta^{18}\text{O}$ content in the snow and interstitial water vapor is elucidated. The
21 observed disequilibrium between snow and vapor isotopes led to exchange of isotopes
22 between snow and vapor under non-equilibrium processes, significantly changing the
23 $\delta^{18}\text{O}$ content of the snow. The type of metamorphism of the snow had a significant
24 influence on this process. These findings are pertinent to the interpretation of the

* Corresponding author. email: schneebeli@slf.ch



25 records of stable isotopes of water from ice cores. These laboratory measurements
26 suggest that a highly resolved history is relevant for the interpretation of the snow
27 isotopic composition in the field.

28

29 *Keywords:* snow, isotope, isothermal, metamorphism, advection, tomography, post-depositional process

30

31 **1. Introduction**

32 Water stable isotopes in polar snow and ice have been used for several decades as
33 proxies for global and local temperatures (e.g. Dansgaard, 1964; Lorius et al., 1979;
34 Grootes et al., 1994; Petit et al., 1999; Johnsen et al., 2001; EPICA Members, 2004).
35 However, the processes that influence the isotopic composition in high-latitude
36 precipitation are complex, making direct inference of paleo temperatures from the
37 isotopic record difficult (Cuffey et al., 1994; Jouzel et al., 1997, 2003; Hendricks et al.,
38 2000). Several factors affect the vapor and snow isotopic composition, which give rise
39 to ice core isotopic composition, starting from the process of evaporation in the source
40 region, until the air mass arrives on top of the ice sheets, and even after snow deposition
41 (Craig and Gordon, 1964; Merlivat and Jouzel, 1979; Johnsen et al. 2001; Ciais and
42 Jouzel, 1994; Jouzel and Merlivat, 1984; Jouzel et al., 2003; Helsen et al., 2005, 2006,
43 2007; Cuffey and Steig, 1998; Krinner and Werner, 2003). Mechanical processes such
44 as mixing, seasonal scouring, or spatial redistribution of snow can alter seasonal and
45 annual records (Fisher et al., 1983; Hoshina et al., 2014). Post-depositional processes
46 associated with wind scouring and snow redistribution are known to introduce a “post-
47 depositional noise” in the surface snow. Comparisons of isotopic records obtained from



48 nearby shallow ice cores have allowed for estimation of a signal-to-noise ratio and a
49 common climate signal (Fisher and Koerner, 1988, 1994; White et al., 1997; Steen-
50 Larsen et al., 2011; Sjolte et al., 2011; Masson-Delmotte et al., 2015). After deposition,
51 interstitial diffusion in the firn and ice affects the water-isotopic signal but back-
52 diffusion or deconvolution techniques have been used to establish the original isotope
53 signal (Johnsen, 1977; Johnsen et al., 2000).

54 The interpretation of ice core data and the comparison with atmospheric model
55 results implicitly rely on the assumption that the snowfall precipitation signal is
56 preserved in the snow-ice matrix (Werner et al. 2011). Classically, ice-core stable-
57 isotope records are interpreted as reflecting precipitation-weighted signals, and
58 compared to observations and atmospheric model results for precipitation, ignoring
59 snow-vapor exchanges between surface snow and atmospheric water vapor (e.g. Persson
60 et al., 2011). However, recent studies carried out on top of the Greenland and Antarctic
61 ice sheets combining continuous atmospheric water vapor isotope observations with
62 daily snow surface sampling document a clear day-to-day variation of isotopic
63 composition of surface snow in-between precipitation events as well as diurnal change
64 in the snow isotopes (Steen-Larsen et al., 2014a; Ritter et al., 2016, Casado et al., 2016).
65 This effect was interpreted as being caused by the uptake of the synoptic-driven
66 atmospheric water-vapor isotope signal by individual snow crystals undergoing snow
67 metamorphism (Steen-Larsen et al., 2014a) and the diurnal variation in moisture flux
68 (Ritter et al., 2016). However, the impact of this process on the isotope-temperature
69 reconstruction is not yet sufficiently understood, but crucial to constrain. This process,
70 compared to interstitial diffusion (Johnsen, 1977; Johnsen et al., 2000), will alter the
71 isotope mean value. The field observations challenge the previous assumption that
72 sublimation occurred molecular layer-by-layer with no resulting isotopic fractionation



73 (Dansgaard, 1964; Friedman et al., 1991; Town et al., 2008; Neumann and Waddington,
74 2004). It is assumed that the solid undergoing sublimation would not be unduly enriched
75 in the heavier isotope species due to the preferential loss of lighter isotopic species to
76 the vapor (Dansgaard, 1964; Friedman et al., 1991). Because self-diffusion in the ice is
77 about three orders of magnitude slower than molecular diffusion in the vapor, the
78 amount of isotopic separation in snow is assumed to be negligible.

79 Snow is a bi-continuous material consisting of fully connected ice crystals and pore
80 space (air) (Löwe et al., 2011). Because of the proximity to the melting point, the high
81 vapor pressure causes a continuous recrystallization of the snow microstructure known
82 as snow metamorphism, even under moderate temperature gradients (Pinzer et al.,
83 2012). The whole ice matrix is continuously recrystallizing by sublimation and
84 deposition, with vapor diffusion as the dominant transport process. Pinzer et al. (2012)
85 showed that a typical half-life of the ice matrix is a few days. The intensity of the
86 recrystallization is dictated by the temperature gradient. Temperature, and geometrical
87 factors (porosity and specific surface area) also play a significant role (Pinzer and
88 Schneebeli, 2009; Pinzer et al., 2012). Snow has a high permeability (Calonne et al.,
89 2012; Zermatten et al., 2014), which facilitates diffusion of gases and, under appropriate
90 conditions, airflow (Gjessing, 1977; Colbeck, 1989; Sturm and Johnson, 1991;
91 Waddington et al., 1996). Modeling of the influence of the so-called ‘wind pumping’-
92 effect (Fisher et al., 1983; Neumann and Waddington, 2004), in which the interstitial
93 water vapor is replaced by atmospheric air pushed through the upper meters of the snow
94 pack by small scale high and low pressure areas caused by irregular grooves or ridges
95 formed on the snow surface (dunes and sastrugi), have assumed that the snow grains
96 would equilibrate with the interstitial water vapor on timescales governed by ice self-
97 diffusion. However, no experimental data are available to support this assumption.



98 With this in mind the experimental study presented here is specifically developed to
99 investigate the effect of ventilation inside the snow pack on the isotopic composition.
100 Only conditions deeper than 1 cm inside a snowpack are considered. Previous work
101 showed that (1) under isothermal conditions, the Kelvin effect leads to a saturation of
102 the pore space in the snow but does not affect the structural change (Ebner et al.,
103 2015a); (2) applying a negative temperature gradient along the flow direction leads to a
104 change in the microstructure due to deposition of water molecules on the ice matrix
105 (Ebner et al., 2015b); and (3) a positive temperature gradient along the flow had a
106 negligible total mass change of the ice but a strong reposition effect of water molecules
107 on the ice grains (Ebner et al., 2016). Here, we measured continuously the isotopic
108 composition of an airflow containing water vapor through a snow sample under both
109 isothermal and temperature gradient conditions. Micro computed-tomography (μ CT)
110 was applied to obtain the 3D microstructure and morphological properties of snow.

111 **2. Experimental setup**

112 Isothermal and temperature gradient experiments with fully saturated airflow and
113 defined isotopic composition were performed in a cold laboratory at around $T_{\text{lab}} \approx -15$
114 $^{\circ}\text{C}$ with small fluctuations of $\pm 0.8 ^{\circ}\text{C}$ (Ebner et al., 2014). Snow produced from de-
115 ionized tap water in a cold laboratory (water temperature: $30 ^{\circ}\text{C}$; air temperature: -20
116 $^{\circ}\text{C}$) was used for the snow sample preparation (Schleef et al., 2014). The snow was
117 sieved with a mesh size of 1.4 mm into a box, and isothermally sintered for 27 days at $-$
118 $5 ^{\circ}\text{C}$ to increase the strength, in order to prevent destruction of the snow sample due to
119 the airflow, and to evaluate the effect of metamorphism of snow. The morphological
120 properties of the snow are listed in Table 1. The sample holder (diameter 53 mm, height
121 30 mm, 0.066 liter) was filled by a cylinder cut out from the sintered snow. To prevent
122 that air can flow between the snow sample and the sample holder walls, the undisturbed



123 snow disk was filled in at a higher temperature (about -5 °C) and sintering was allowed
124 for about 1 h before cooling down and start of the experiment. The setup of Ebner et al.
125 (2014) was modified by additionally inserting a water vapor isotope analyzer (Model:
126 L1102-I Picarro, Inc., Santa Clara, CA, USA) to measure the isotopic ratio $\delta^{18}\text{O}$ of the
127 water vapor contained in the airflow at the inlet and outlet of the sample holder. The
128 experimental setup consisted of three main components (humidifier, sample holder, and
129 the Picarro analyzer) were connected with insulated copper tubing and Swagelok fitting
130 (Fig. 1). The tubes to the Picarro analyzer were heated to prevent deposition of water
131 vapor and thereby fractionation. The temperature was monitored with thermistors inside
132 the humidifier and at the inlet and outlet of the snow sample. A dry air pressure tank
133 controlled by a mass flow controller (EL-Flow, Bronkhorst) generated the airflow. A
134 humidifier, consisting of a tube (diameter 60 mm, height 150 mm, 0.424 liter volume)
135 filled with crushed ice particles (snow from Antarctica with low $\delta^{18}\text{O}$ composition), was
136 used to saturate the dry air entering the humidifier with water vapor at an almost
137 constant isotopic composition. The air temperature in the humidifier and at the inlet of
138 the snow sample was maintained at the same value (accuracy ± 0.2 K) to limit changes
139 influence of variability in absolute vapor pressure and isotopic composition. We
140 measured the $\delta^{18}\text{O}$ of the water vapor produced by the humidifier before and after each
141 experimental run ($\delta^{18}\text{O}_{\text{hum}}$). The outlet flow ($\delta^{18}\text{O}_{\text{a}}$) of the sample holder was
142 continuously measured during the experiment to analyze the temporal evolution of the
143 isotopic signal. All data from the Picarro analyzer were corrected to the humidity
144 reference level using the established instrument humidity-isotope response (2013;
145 2014b). In addition, VSMOW-SLAP correction and drift correction were performed.
146 We followed the calibration protocol and used the calibration system described in detail
147 by Steen-Larsen et al. (2013; 2014b).



148 The sample holder described by Ebner et al. (2014) was used because it already had
149 the appliance to analyze the snow by μ CT. Tomography measurements were performed
150 with a modified μ -CT80 (Scanco Medical). The equipment incorporated a microfocus
151 X-ray source, operated at 70 kV acceleration voltage with a nominal resolution of 18
152 μ m. The samples were scanned with 1000 projections per 180° in high-resolution
153 setting, with typical adjustable integration time of 200 ms per projection. The field of
154 view of the scan area was 36.9 mm of the total 53 mm diameter, and subsamples with a
155 dimension of $7.2 \times 7.2 \times 7.2$ mm³ were extracted for further processing. The
156 reconstructed μ CT images were filtered using a $3 \times 3 \times 3$ median filter followed by a
157 Gaussian filter ($\sigma = 1.4$, support = 3). The Otsu method (Otsu, 1979) was used to
158 automatically perform clustering-based image thresholding to segment the grey-level
159 images into ice and void phase. Morphological properties in the two-phase system were
160 determined based on the exact geometry obtained by the μ CT. Tetrahedrons
161 corresponding to the enclosed volume of the triangulated ice matrix surface were
162 applied on the segmented data to determine porosity (ε) and specific surface area (SSA).
163 Opening size distribution operation was applied in the segmented μ CT data to extract
164 the mean pore size (d_{mean}) (Haussener et al., 2012).

165 Three experiments with saturated advective airflow through the snow sample were
166 performed to record the following parameters and analyze their effects: (1) isothermal
167 conditions to analyze the influence of curvature effects (Kaempfer al et., 2007); (2)
168 positive temperature gradient applied to the snow sample where cold air is heated up
169 while flowing through the sample in order to analyze the influence of sublimation; (3)
170 negative temperature gradient applied to the snow sample where warm air is cooled
171 down while flowing across the sample, to analyze the influence of net deposition.
172 During the temperature gradient experiments, a temperature difference of 1.4 °C and 1.8



173 $^{\circ}\text{C}$ was imposed resulting in a gradient of $+47 \text{ K m}^{-1}$ and -60 K m^{-1} , respectively. The
174 runs were performed at atmospheric pressure and with a volume flow rate of 3.0 liter
175 min^{-1} corresponding to an average flow speed in the pores of $\approx 30 \text{ mm s}^{-1}$. In experiment
176 (2) the outlet temperature and in experiment (3) the inlet and also the humidifier
177 temperature was actively controlled using thermo-electric elements. Variations in
178 temperature of up to $\pm 0.8 \text{ }^{\circ}\text{C}$ were due to temperature fluctuations inside the cold
179 laboratory, leading to slightly variable temperature gradients and mean temperature in
180 experiment (2) and (3). Table 1 presents a summary of the experimental conditions and
181 the morphological properties of the snow samples. At the end of each experiment, the
182 snow sample was cut into five layers of 6 mm height and the isotopic composition of
183 each layer was analyzed to examine the spatial $\delta^{18}\text{O}$ gradient in the isotopic composition
184 of the snow sample.

185 A slight increase with a maximum of 0.7 ‰ of $\delta^{18}\text{O}$ in the water vapor produced by
186 the humidifier was observed during the experiments (Table 2). This change of $\sim 0.7\text{‰}$ is
187 not significant compared to the difference between the isotopic composition of the water
188 vapor and the snow sample in the sample holder of $\sim 53\text{‰}$ and the temporal change of
189 the water vapor isotopes on the back side of the snow sample.

190 **3. Results**

191 **3.1 Isothermal condition**

192 The experiment (1) was performed for 24 h at a mean temperature of $T_{\text{mean}} = -15.5$
193 $^{\circ}\text{C}$. $\delta^{18}\text{O}_a$ decreased exponentially in the outlet flow was observed throughout the
194 experimental run as shown in Fig. 2. Initially, the $\delta^{18}\text{O}_a$ content in the flow was -27.7 ‰
195 and exponentially decreased to -47.6 ‰ after 24 h. The increase of $\delta^{18}\text{O}_a$ in the first
196 approximately 30 min was due to memory effects from air and possible condensed



197 water left in the tubes from a prior experiment. The small fluctuations in the $\delta^{18}\text{O}_a$
198 signal at $t \approx 7$ h, 17 h and 23 h were due to small temperature changes in the cold
199 laboratory.

200 We observed a strong interaction between the airflow and the snow was observed in
201 the isotopic composition of the snow. The $\delta^{18}\text{O}_s$ signal in the snow decreased by 4.75 –
202 7.78 ‰ and an isotopic gradient in the snow was observed after the experimental run,
203 shown in Fig. 3. Initially, the snow had a homogeneous isotopic composition of $\delta^{18}\text{O}_s =$
204 -10.97 ‰ but post-experiment sampling showed a decrease in the snow $\delta^{18}\text{O}$ at the inlet
205 side to -17.75 ‰ and at the outlet side to -15.72 ‰. The spatial $\delta^{18}\text{O}_s$ gradient of the
206 snow had an approximate slope of 0.68 ‰ mm⁻¹ at the end of the experimental run.
207 Table 2 shows the $\delta^{18}\text{O}$ value in snow at the beginning ($t = 0$) and end ($t = 24$ h) of the
208 experiment.

209 **3.2 Air warming by a positive temperature gradient along the airflow**

210 The experiment (2) was performed over a period of 24 h with an average
211 temperature gradient of approximatively +47 K m⁻¹ (warmer temperatures at the outlet
212 of the snow) and an average mean temperature of -14.7 °C. We observed again a
213 relaxing exponential decrease of $\delta^{18}\text{O}_a$ in the outlet flow was observed throughout the
214 measurement period as shown in Fig. 2, but the decrease was slower compared to the
215 isothermal run. Initially, the $\delta^{18}\text{O}_a$ content in the flow coming through the snow disk
216 was -29.8 ‰ and exponentially decreased to -41.9 ‰ after 24 h. The increase of $\delta^{18}\text{O}_a$
217 in the first 30 min was due to memory effects as explained previously. The small
218 fluctuations in the $\delta^{18}\text{O}_a$ signal at $t \approx 2.7$ h, and 12.7 h were due to small temperature
219 changes in the cold laboratory.

220 The $\delta^{18}\text{O}_s$ signal in the snow decreased up to 4.66 – 7.66 ‰ and a gradient in
221 isotopic composition of the snow was observed after the experimental run, shown in



222 Fig. 3. Initially, the snow had a homogeneous isotopic composition of $\delta^{18}\text{O}_s = -11.94$
223 ‰, but post-experiment sampling showed a decrease at the inlet side to -19.6 ‰ and at
224 the outlet side to -16.6 ‰. The spatial $\delta^{18}\text{O}_s$ gradient of the snow had an approximate
225 slope of 1.0 ‰ mm⁻¹ at the end of the experimental run. Table 2 shows the $\delta^{18}\text{O}_s$ value
226 in snow at the beginning ($t = 0$) and end ($t = 24$ h) of the experiment.

227 **3.3 Air cooling by a negative temperature gradient along the air flow**

228 The experiment (3) was performed for 84 h instead of 24 h to better estimate the
229 trend in $\delta^{18}\text{O}_a$ in the outlet flow. An average temperature gradient of approximately -60
230 K m⁻¹ (colder temperatures at the outlet of the snow) and an average mean temperature
231 of -13.2 °C were observed during the experiment. As in the previous experiments, a
232 relaxing exponential decrease of $\delta^{18}\text{O}_a$ in the outlet flow was observed throughout the
233 experimental run as shown in Fig. 2, but the decrease was slower compared to the
234 isothermal run and temperature gradient opposed to the airflow. Initially, the $\delta^{18}\text{O}_a$
235 content in the flow was -29.8 ‰ and exponentially decreased to -37.7 ‰ after 84 h. The
236 increase of $\delta^{18}\text{O}_a$ in the first 30 min was again due to memory effects. The small
237 fluctuations in the $\delta^{18}\text{O}_a$ signal at $t \approx 7.3$ h, 21.3 h, 31.3 h, 45.3 h, 55.3 h, 69.3 h, and
238 79.3 h were due to small temperature changes in the cold laboratory.

239 The $\delta^{18}\text{O}_s$ signal in the snow decreased up to 4.46 – 15.09 ‰ and a gradient in the
240 isotopic composition of the snow was observed after the experimental run, shown in
241 Fig. 3. Initially, the snow had an isotopic composition of $\delta^{18}\text{O}_s = -10.44$ ‰ but post-
242 experiment sampling showed a decrease at the inlet side to -25.53 ‰ and at the outlet
243 side to -15.00 ‰. The spatial $\delta^{18}\text{O}_s$ gradient of the snow had an approximate slope of
244 3.5 ‰ mm⁻¹ at the end of the experimental run. Table 2 shows the $\delta^{18}\text{O}_s$ value in snow
245 at the beginning ($t = 0$) and end ($t = 84$ h) of the experiment.



246 **4. Discussion**

247 All experiments showed a strong exchange in $\delta^{18}\text{O}$ between the snow and water-
248 vapor saturated air resulting in a significant change of the value of the stable isotopes in
249 the snow. The advective conditions in the experiments were comparable with surface
250 snow layers in Antarctica and Greenland, but at higher temperature, especially
251 compared to interior Antarctica. In wind pumping theory, an airflow velocity of $u_D \approx 10$
252 mm s^{-1} (corresponding Reynolds number $Re \approx 0.65$) was estimated inside the surface
253 snow layers ($d_{\text{mean}} \approx 1 \text{ mm}$) for a high wind speed above the snow surface ($\approx 10 \text{ m s}^{-1}$)
254 (Neumann, 2003). We performed experiments with airflow velocities inside the snow
255 sample of around 30 mm s^{-1} (corresponding Reynolds number $Re = 0.7$), which was a
256 factor three higher than in natural conditions, but still in the feasible flow regime
257 according to the Reynolds number.

258 The results also showed strong interactions in $\delta^{18}\text{O}$ between snow and air depending
259 on the different temperature gradient conditions. The experiments indicate that
260 temperature variation and airflow above and through the snow structures (Sturm and
261 Johnson, 1991; Colbeck, 1989; Albert and Hardy, 1995) seem to be dominant processes
262 affecting water stable isotopes of surface snow. In a typical Antarctic and Greenland
263 snow profile, strong interactions between the atmosphere and snow occurs, especially in
264 the first 2 m (Neumann and Waddington, 2004; Town et al., 2008), called the
265 convective zone. In the convective zone, air can move relatively freely and therefore
266 exchange between snow and the atmospheric air occurs. Air flowing into the snow
267 reaches saturation vapor pressure nearly instantly through sublimation (Neumann et al.,
268 2008; Ebner et al., 2015a). Our results support the interpretation that changes in surface
269 snow isotopic composition are expected to be significant if large day-to-day surface
270 changes in water vapor occur in between precipitation events, wind pumping is efficient



271 and snow metamorphism is enhanced by temperature gradients in the upper first
272 centimeters of the snow (Steen-Larsen et al., 2014a).

273 We expect that our findings will lead to influence the interpretation of the water
274 stable isotope records from ice cores. Classically, ice core stable isotope records are
275 interpreted as paleo-temperature reflecting precipitation-weighted signals. When
276 comparing observations and atmospheric model results for precipitation with ice core
277 records, such vapor-snow exchanges are normally ignored (e.g. Persson et al. (2011)
278 and Fujita and Abe (2006)). However, vapor-snow exchange enhanced by
279 recrystallization rate seems to be an important factor for the high variation in the snow
280 surface $\delta^{18}\text{O}$ signal as supported by our experiments. It was hypothesized that the
281 changes in the snow-surface $\delta^{18}\text{O}$ reported by Steen-Larsen et al. (2014a) are caused by
282 changes in large-scale wind and moisture advection of the atmospheric water vapor
283 signal and snow metamorphism. The strong interaction between atmosphere and near-
284 surface snow can modify the ice core water stable isotope records.

285 The rate-limiting step for isotopic exchange in the snow is isotopic equilibration
286 between the pore-space vapor and surrounding ice grains. The relaxing exponential
287 decrease of $\delta^{18}\text{O}$ in the outflow of our experiments predicted that full isotopic
288 equilibrium between snow and atmospheric vapor will not be reached at any depth
289 (Waddington et al., 2002; Neumann and Waddington, 2004) but changes towards
290 equilibrium with the atmospheric state occurs, effectively changing the “target” towards
291 which the snow is equilibrating (Steen-Larsen et al., 2013, 2014a).

292 As snow accumulates, the upper 2 m are advected through the ventilated zone
293 (Neumann and Waddington, 2004; Town et al., 2008). In areas with high accumulation
294 rate (e.g. South Greenland), snow is advected for a short time through the ventilated
295 zone. Relatively short time vapor snow exchange would result in higher spatial



296 variability compared to long-time. However, the effects of snow ventilation on isotopic
297 composition may become more important as the accumulation rate of the snow
298 decreases ($< 50 \text{ mm a}^{-1}$), such that snow remains in the near-surface ventilated zone for
299 many years (Waddington et al., 2002; Hoshina et al., 2014; Hoshina et al., 2016). As the
300 snow remains longer in the near-surface ventilated zone, a larger $\delta^{18}\text{O}$ exchange
301 between snow and atmospheric vapor will occur. Consequently, the isotopic content of
302 layers at sites with high and low accumulation rates can evolve differently, even if the
303 initial snow composition had been equal, and the sites had been subjected to the same
304 histories of air-mass vapor.

305 We now discuss the fact that despite a relatively small change in the difference
306 between the isotopic composition of the incoming vapor and the snow, large differences
307 in the isotopic composition of the water vapor at the outlet flow exist for the three
308 different experimental setups. Based on the difference in the outlet water vapor isotopic
309 composition, we hypothesized that different processes are at play for the different
310 experiments. It is obvious that there is a fast isotopic exchange with the surface of the
311 ice crystals, and a much slower timescale on which the interior of the ice crystals gets
312 altered. Due to the low diffusivity of H_2^{16}O and H_2^{18}O in ice ($D_{\text{H}_2^{18}\text{O}} \approx D_{\text{H}_2^{16}\text{O}} = \sim 10^{-15}$
313 $\text{m}^2 \text{ s}^{-1}$ (Ramseier, 1967; Johnsen et al., 2000)), we assumed that the interior is not
314 altered on the timescale of the experiment. This explained why the net isotopic change
315 of the bulk sample is relatively small compared to the changes in the outlet water vapor
316 isotopes. The effective ‘ice-diffusion depth’ of the isotopic exchange during the
317 experiments is given as $L_D = \sqrt{D \cdot t}$, where D is the diffusion coefficient of H_2^{16}O and
318 H_2^{18}O in ice, respectively, and t the experimental time. The calculated ‘ice-diffusion
319 depth’ L_D , is $\sim 9.3 \mu\text{m}$ for experiment (1) and (2), and $\sim 17.4 \mu\text{m}$ for experiment (3),
320 respectively, indicating an expected low altering of the interior of the ice crystal.



321 However, snow has a large specific surface area and therefore a high exchange area.
322 This has an effect on the $\delta^{18}\text{O}$ snow concentration. The fraction of the total volume V_{tot}
323 of ice that is close enough to the ice surface to be affected by diffusion in time t is then
324 $\rho_{\text{ice}} \cdot \text{SSA} \cdot L_{\text{D}}$, where SSA is the specific surface area (area per unit mass), and L_{D} is
325 the diffusion depth (above) for time t . For $t \approx 24$ hours, a large fraction (24 to 43 %) the
326 total volume V_{tot} of the ice matrix can be accessed through diffusion. It is quite hard to
327 see the total $\delta^{18}\text{O}$ snow difference between experiments (1) and (2) after the experiment
328 compared to the $\delta^{18}\text{O}$ of the vapor in the air at the outlet. But there is still a notable
329 effect in the $\delta^{18}\text{O}$ of the snow between experiment (1) and (2). Due to the higher
330 recrystallization rate of experiment (2) the spatial $\delta^{18}\text{O}_s$ gradient of the snow (1.0 ‰
331 mm^{-1}) is higher than for experiment (1) (0.68 ‰ mm^{-1}). Increasing the experimental
332 time, the $\delta^{18}\text{O}$ change in the snow increases (experiment (3)). In general, the calculated
333 ‘ice-diffusion depth’ is realistic under isothermal conditions where diffusion processes
334 are the main factors (Kaempfer and Schneebeli, 2007; Ebner et al., 2015). Applying a
335 temperature gradient, the impact of diffusion is suppressed due to the high
336 recrystallization rate by sublimation and deposition. Due to the low half-life of the ice
337 matrix of a few days, the growth rates are typically on the order of 100 μm per day
338 (Pinzer et al., 2012). Therefore, this redistribution of ice counteracts the diffusion into
339 the solid ice.

340 By comparing similarities and differences between the outcomes of the three
341 experimental setups we will now discuss the physical processes influencing the
342 interaction and exchange processes within the snowpack between the snow and the
343 advected vapor. We first notice that the final snow isotopic profile of experiment (1)
344 (isothermal) and (2) (positive temperature gradient along the direction of the flow) are
345 comparable to each other. Despite this similarity, the evolution in the outlet water vapor



346 of experiment (1) showed a significantly stronger depletion compared to experiment (2).
347 For experiment (3) (negative temperature gradient along the direction of the flow) we
348 observed the smallest change in outlet water vapor isotopes but the largest snow-pack
349 isotope gradient after the experiment. However, this change was caused by 84 hours
350 flow instead of 24 hours.

351 Curvature effects, temperature gradients and therefore the recrystallization rate
352 influence the mass transfer of $H_2^{16}O$ / $H_2^{18}O$ molecules. The higher the recrystallization
353 rate of the snow the slower the adaption of the outlet air concentration to the inlet air
354 concentration (see in experiment (2) and (3)). Under isothermal conditions (experiment
355 (1)) the only effect influencing the recrystallization rate is the curvature effect
356 (Kaempfer and Schneebeli, 2007). However, based on the experimental observations
357 (Kaempfer and Schneebeli, 2007) this effect decreases with decreasing temperature and
358 increasing experimental time. Applying an additional temperature gradient on a snow
359 sample, there are complex interplays between local sublimation and deposition on
360 surfaces and the interaction of water molecules in the air with the ice matrix due to
361 changing saturation conditions of the airflow. Therefore, the recrystallization rate
362 increases and thus the change in the $\delta^{18}O$ of the air. For experiment (2) there is a
363 complex interplay between sublimation and deposition of water molecules into the
364 interstitial flow (Ebner et al., 2015c) while for experiment (3) there are deposition of
365 molecules carried by the interstitial flow onto the snow crystals (Ebner et al., 2015b).
366 Furthermore, in the beginning of each experiment there is a tendency to sublimate from
367 edges of the individual snow crystals due to the higher curvature. As the edges were
368 sublimated and deposition occurred in the concavities, the individual snow crystals
369 became more rounded, slowing down the transfer of water molecules into the interstitial
370 airflow. We noticed for all three experiments that within the uncertainty of the isotopic



371 composition of the snow, the initial isotopic composition of the vapor was the same and
372 in isotopic equilibrium with the snow. The difference between experiment (1) and (2)
373 lies in the fact that due to the temperature gradient in experiment (2) there is an
374 increased transfer of water vapor with the isotopic composition of the snow in to the
375 airflow. Hence the depleted air from the humidifier advected through the snow disk is
376 mixed with a relatively larger vapor flux from the snow crystals. Additionally, we also
377 expected less deposition into the concavities in experiment (2) compared to experiment
378 (1). However, it is interesting to note that the final isotopic profile of the snow disk is
379 similar in experiment (1) and experiment (2). We interpreted this as being a result of
380 two processes acting in opposite direction: although relatively isotope-depleted vapor
381 from the humidifier was deposited on the ice matrix there was also a higher amount of
382 sublimation of relatively isotope-enriched vapor from the snow disk in experiment (2).
383 Experiment (3) separates itself from the other two experiments in the way that as the
384 water vapor from the humidifier is advected through the snow disk there is a continuous
385 deposition of very depleted air due the negative temperature gradient. As for the case of
386 experiment (1) and (2) there was also in experiment (3) a constant sublimation of the
387 convexities into the vapor stream. We notice that despite the fact that experiment 3 ran
388 for 84 hours the snow at the outlet side of the snow-disk did not become more
389 isotopically depleted compared to experiment (1) and (2). However, the snow on the
390 inlet side became significantly more isotopically depleted. By having this observation in
391 mind, together with the fact that the vapor of the outlet of the snow-disk is less depleted
392 compared to experiment (1) and (2), lead us to hypothesize that there is a relatively
393 larger deposition of isotopically depleted vapor from the humidifier as the vapor is
394 advected through the snow disk. This means that a relatively larger component of the



395 isotopic composition of the vapor is originating by sublimation from the convexities of
396 the snow disk and less from the isotopically depleted vapor from the humidifier.

397 Our hypotheses ask for additional validation by more detailed experiments.
398 Specifically, it would be crucial to know the mass balance of the snow disk more
399 precisely, which could be done by scanning the entire snow disk following the change
400 in density and morphological properties over the entire height, or gravimetrically.
401 Insights would also be achieved with experiments using snow of the same isotopic
402 composition, but different SSA, as this would allow calculating more precisely the
403 different observed exchange rates. Additionally, different and colder background
404 temperatures should be tested to better understand inland Antarctic environment and the
405 effect of the quasi-liquid layer, which is necessary for the development of a numerical
406 model. Isotopically different combinations of vapor and snow should be performed. In
407 the present manuscript, vapor with low $\delta^{18}\text{O}$ isotopic composition was transported
408 through snow with relative high $\delta^{18}\text{O}$ isotopic composition. It would be interesting to
409 reverse the combination and perform experiments with different combinations to
410 provide more insights on mass and isotope exchanges between vapor and snow.
411 Experiments with longer running time helps to understand the change in the ice matrix
412 better. Further, as in the humidifier we had not only sublimation but a complex interplay
413 of simultaneously sublimation and deposition due to the geometrical complexity of
414 snow, a further experiment is suggested to show isotopic fractionation during
415 sublimation. Dry air is blown over a flat ice surface and is immediately removed. With
416 the suggested experiment the actual statement whether there is no measurable
417 fractionation and the sublimated vapor has the same $\delta^{18}\text{O}$ value as the sublimating ice or
418 not can be proved. Based on the results of this paper, we expect a different $\delta^{18}\text{O}$ value
419 between vapor and ice, especially at the beginning (see Fig. 4). Due to the fact that



420 $H_2^{16}O$ is lighter in mass than $H_2^{18}O$, the energy required to change the state from solid
421 to vapor is less. Therefore, especially at the beginning of the experiment, the vapor is
422 depleted in $H_2^{18}O$ and thus a different $\delta^{18}O$ value in the vapor and ice should be seen.
423 After a while the ice interface is depleted in $H_2^{16}O$ molecules and because the self-
424 diffusion in ice is low, an approach of the $\delta^{18}O$ value of the vapor and ice should be
425 seen. Comparing the penetration depths for diffusion ($L_D = \sqrt{D \cdot t}$; where $D \approx 10^{-15} \text{ m}^2 \text{ s}^{-1}$)
426 and for sublimation ($L_{\text{sub}} = v_{\text{sub}}t$; where $v_{\text{sub}} \approx 100 \text{ } \mu\text{m per day}$ (Pinzer et al., 2012))
427 the time $t = D/v_{\text{sub}} \approx 10^3 \text{ s}$ represents the transition from diffusion-dominated behavior
428 (with fractionation on sublimation) to sublimation-dominated behavior (in which nearly
429 all $H_2^{18}O$ atoms are forced to enter the vapor phase). This is obviously not a precise
430 number but it suggests that after about 10^3 seconds, sublimation from the ice crystals
431 occurs without significant isotopic fractionation. However, as we have not performed
432 such experiments yet, these statements are only speculative.

433 **4. Summary and conclusion**

434 We analyzed the influence of airflow and metamorphism across a snow sample on
435 the $\delta^{18}O$ isotopic composition in controlled laboratory experiments. Three experiments
436 with saturated advective airflow across the snow sample with a volume flow rate of $3.0 \text{ liter min}^{-1}$ ($u_D \approx 3 \text{ cm s}^{-1}$)
437 were performed: (1) isothermal run to analyze the influence of the curvature effects; (2) positive temperature gradient run (approx. $+47 \text{ K m}^{-1}$) along
438 the airflow where cold air heated up while flowing through the sample to analyze the
439 influence of net ice mass loss in a snowpack; and (3) negative temperature gradient run
440 (approx. -60 K m^{-1}) where warm air cooled down while flowing through the sample, to
441 analyze the influence of deposition. Air with low $\delta^{18}O$ content ($-68 \text{ } \text{\textperthousand} - -62 \text{ } \text{\textperthousand}$) was
442 blown into the snow sample and the $\delta^{18}O$ outlet was continuously measured with a



444 water vapor isotope analyzer. The $\delta^{18}\text{O}$ distribution through the snow disk was
445 measured at the beginning and end of each experiment. μCT measurements were
446 applied to obtain the 3D microstructure and the morphological properties, namely:
447 porosity (ε), specific surface area (SSA), and the mean pore size (d_{mean}) of the snow.

448 Laboratory experimental runs were performed where a transient $\delta^{18}\text{O}$ interaction
449 between snow and air was observed. The airflow altered the isotopic composition of the
450 snowpack and supports an improved climatic interpretation of ice core stable water
451 isotope records. The water vapor saturated airflow with an isotopic difference of up to
452 55‰ changed within 24 h and 84 h the original $\delta^{18}\text{O}$ isotope signal in the snow by up to
453 7.64 ‰ and 15.06 ‰. The disequilibrium between snow and air isotopes led to the
454 observed exchange of isotopes, the rate depending on the temperature gradient
455 conditions. Concluding, increasing the recrystallization rate in the ice matrix the
456 temporal change of the $\delta^{18}\text{O}$ concentration at the outflow decreases (experiment (2) and
457 (3)). Decreasing the recrystallization rate the temporal curve of the outlet concentration
458 is getting steeper reaching the $\delta^{18}\text{O}$ inlet concentration of the air faster (experiment (1)).

459 Additionally, the complex interplay of simultaneous diffusion, sublimation and
460 deposition due to the geometrical complexity of snow has a strong effect on the $\delta^{18}\text{O}$
461 signal in the snow and cannot be neglected. A temporal signal can be superimposed on
462 that cloud-temperature signal, (a) if the snow remains near the surface for a long time,
463 i.e. in a low-accumulation area, and (b) is exposed to a history of air masses carrying
464 vapor with a significantly different isotopic signature than the precipitated snow.

465 These are novel measurements and will therefore be important for allowing other
466 researchers formulate their research question based on and carry out further
467 experiments. Our results represent the first direct experimental observation showing
468 interaction between the water isotopic composition of the snow, the water vapor in the



469 air and recrystallization due to temperature gradients. Previous work on isotopic content
470 of surface snow failed to incorporate the recrystallization process, and recrystallization
471 and bulk mass exchange must be incorporated into future models of snow and firn
472 evolution. Further studies are required on the influence of temperature and airflow as
473 well as snow microstructure on the mass transfer phenomena for validating the
474 implementation of stable water isotopes in snow models.

475

476

477 **Acknowledgements**

478 The Swiss National Science Foundation granted financial support under project Nr.
479 iso. H.C. Steen-Larsen was supported by the AXA Research Fund. The authors thank K.
480 Fujita, E. D. Waddington and an anonymous reviewer for the suggestions and critical
481 review. M. Jaggi, S. Grimm, A. Schlumpf, and S. Berben gave technical support. The
482 data for this paper are available by contacting the corresponding author.

483

484 **References**

485 Albert M. R. and Hardy J. P.: Ventilation experiments in a seasonal snow cover, in
486 Biogeochemistry of Seasonally Snow-Covered Catchments, IAHS Publ. 228, edited
487 by K. A. Tonnesen, M. W. Williams, and M. Tranter, 41–49, IAHS Press,
488 Wallingford, UK, 1995.

489 Calonne N., Geindreau C., Flin F., Morin S., Lesaffre B., Rolland du Roscoat S., and
490 Charrier P.: 3-D image-based numerical computations of snow permeability: links
491 to specific surface area, density, and microstructural anisotropy, *The Cryosphere*, 6,
492 939–951, 2012.



493 Casado M., Landais A., Masson-Delmotte V., Genthon C., Kerstel E., Kassi S., Arnaud
494 L., Picard G., Prie F., Cattani O., Steen-Larsen H. C., Vignon E., and Cermak P.:
495 Continuous measurements of isotopic composition of water vapour on the East
496 Antarctic Plateau, *Atmos. Chem. Phys. Discuss.*, doi:10.5194/acp-2016-8, in
497 review, 2016.

498 Ciais P., and Jouzel J.: Deuterium and oxygen 18 in precipitation: Isotopic model,
499 including mixed-cloud processes, *Journal of Geophysical Research*, 99, 16793–
500 16803, doi:10.1029/94JD00412, 1994.

501 Colbeck S. C.: Air movement in snow due to windpumping, *Journal of Glaciology*, 35,
502 209–213, 1989.

503 Craig H. and Gordon L. I.: Deuterium and oxygen 18 variations in the ocean and marine
504 atmosphere, In proc. Stable Isotopes in Oceanographic Studies and
505 Paleotemperatures, (ed. E. Toniorgi), Spoleto, Italy, 9–130, 1964.

506 Cuffey K. M. and Steig E. J.: Isotopic diffusion in polar firn: Implications for
507 interpretation of seasonal climate parameters in ice-core records, with emphasis on
508 central Greenland, *Journal of Glaciology*, 44, 273–284, 1998.

509 Cuffey K. M., Alley R. B., Grootes P. M., Bolzan J. M., and Anandakrishnan S.:
510 Calibration of the Delta-O-18 isotopic paleothermometer for central Greenland,
511 using borehole temperatures, *Journal of Glaciology*, 40, 341–349, 1994.

512 Dansgaard W.: Stable isotopes in precipitation, *Tellus*, 16, 436–468, 1964.

513 Ebner P. P., Grimm S., Schneebeli M., and Steinfeld A.: An instrumented sample holder
514 for time-lapse micro-tomography measurements of snow under advective
515 conditions, *Geoscientific Instrumentation Methods and Data Systems*, 3, 179–185,
516 doi:10.5194/gi-3-179-2014, 2014.



517 Ebner P. P., Schneebeli M., and Steinfeld A. Tomography-based observation of
518 isothermal snow metamorphism under advective conditions, *The Cryosphere*, 9,
519 1363–1371, 2015a.

520 Ebner P. P., Andreoli C., Schneebeli M., and Steinfeld A.: Tomography-based
521 characterization of ice-air interface dynamics of temperature gradient snow
522 metamorphism under advective conditions, *Journal of Geophysical Research*,
523 *Journal of Geophysical Research Earth Surface*, 120, doi:10.1002/2015JF003648,
524 2015b.

525 Ebner P. P., Schneebeli M., and Steinfeld A.: Metamorphism during temperature
526 gradient with undersaturated advective airflow in a snow sample, *The Cryosphere*,
527 10, 791–797, 2016.

528 EPICA Members: Eight glacial cycles from an Antarctic ice core, *Nature*, 429, 623–
529 628, doi:10.1038/nature02599, 2004.

530 Gjessing Y. T.: The filtering effect of snow, in: *Isotopes and Impurities in Snow and Ice*
531 Symposium, edited by: Oeschger, H., Ambach, W., Junge, C. E., Lorius, C., and
532 Serebryanny, L., IASHAISH Publication, Dorking, 118, 199–203, 1977.

533 Grootes P. M., Steig E., and Stuiver M.: Taylor Ice Dome study 1993–1994: An ice core
534 to bedrock, *Antarctic Journal U.S.*, 29, 79–81, 1994.

535 Fisher D. A., Koerner R. M., Paterson W. S. B., Dansgaard W., Gundestrup N., and
536 Reeh N.: Effect of wind scouring on climatic records from ice-core oxygen-isotope
537 profiles, *Nature*, 301, 205–209, doi:10.1038/301205a0, 1983.

538 Fisher D. A. and Koerner R.: The effect of wind on $d(18O)$ and accumulation given an
539 inferred record of seasonal d amplitude from the Agassiz ice cap, Ellesmere island,
540 Canada, *Annals of Glaciology*, 10, 34–37, 1988.



541 Fisher D. A. and Koerner R.: Signal and noise in four ice-core records from the Agassiz
542 ice cap, Ellesmere Island, Canada: Details of the last millennium for stable
543 isotopes, melt and solid conductivity, *The Holocene*, 4, 113–120,
544 doi:10.1177/095968369400400201, 1994.

545 Friedman I., Benson C., and Gleason J.: Isotopic changes during snow metamorphism,
546 in *Stable Isotope Geochemistry: A Tribute to Samuel Epstein*, edited by J. R.
547 O'Neill and I. R. Kaplan, pp. 211–221, Geochemical Society, Washington, D. C.,
548 1991.

549 Haussener S., Gergely M., Schneebeli M., and Steinfeld A.: Determination of the
550 macroscopic optical properties of snow based on exact morphology and direct pore-
551 level heat transfer modeling, *Journal of Geophysical Research*, 117, 1–20,
552 doi:10.1029/2012JF002332, 2012.

553 Helsen M. M., van de Wal R. S. W., van den Broeke M. R., van As D., Meijer H. A. J.,
554 and Reijmer C. H.: Oxygen isotope variability in snow from western Dronning
555 Maud Land, Antarctica and its relation to temperature, *Tellus*, 57, 423–435, 2005.

556 Helsen M. M., van de Wal R. S. W., van den Broeke M. R., Masson-Delmotte V.,
557 Meijer H. A. J., Scheele M. P., and Werner M., Modeling the isotopic composition
558 of Antarctic snow using backward trajectories: Simulation of snow pit records,
559 *Journal of Geophysical Research*, 111, doi:10.1029/2005JD006524, 2006.

560 Helsen M. M., van de Wal R. S. W., and van den Broeke M. R.: The isotopic
561 composition of present-day Antarctic snow in a Lagrangian simulation, *Journal of
562 Climate*, 20, 739–756, 2007.

563 Hendricks M. B., DePaolo D. J., and Cohen R. C.: Space and time variation of $\delta^{18}\text{O}$ and
564 δD in precipitation: Can paleotemperature be estimated from ice cores?, *Global
565 Biogeochemical Cycles*, 14, 851–861, doi:10.1029/1999GB001198, 2000.



566 Hoshina Y., Fujita K., Nakazawa F., Iizuka Y., Miyake T., Hirabayashi M., Kuramoto
567 T., Fujita S., and Motoyama H.: Effect of accumulation rate on water stable
568 isotopes of near-surface snow in inland Antarctica. *Journal of Geophysical*
569 *Research - Atmospheres*, 119(1), 274-283. doi:10.1002/2013JD020771, 2014.

570 Hoshina Y., Fujita K., Iizuka Y., Motoyama H.: Inconsistent relations among major ions
571 and water stable isotopes in Antarctica snow under different accumulation
572 environments. *Polar Science*, 10, doi:10.1016/j.polar.2015.12.003, 2016.

573 Johnsen S. J.: Stable isotope homogenization of polar firn and ice, in *Isotopes and*
574 *Impurities in Snow and Ice, Proceeding of the Grenoble Symposium*,
575 August/September 1975, 210–219, IAHS AISH Publication, 118, Grenoble, France,
576 1997.

577 Johnsen S. J., Clausen H. B., Cuffey K. M., Hoffman G., Schwander J., and Creyts T.:
578 Diffusion of stable isotopes in polar firn and ice: The isotope effect in firn
579 diffusion, in *Physics of Ice Core Records*, edited by T. Honda, 121–140,
580 Hokkaido University Press, Sapporo, Japan, 200.

581 Johnsen S. J., Dahl-Jensen D., Gundestrup N., Steffensen J. P., Clausen H. B., Miller
582 H., Masson-Delmotte V., Sveinbjörnsdóttir A. E., and White J.: Oxygen isotope
583 and palaeotemperature records from six Greenland ice-core stations: Camp
584 Century, DYE-3, GRIP, GISP2, Renland and NorthGRIP, *Journal of Quaternary*
585 *Science*, 16, 299–307, doi:10.1002/jqs.622, 2001.

586 Jouzel J. and Merlivat L.: Deuterium and oxygen 18 in precipitation: Modeling of the
587 isotopic effects during snow formation, *Journal of Geophysical Research*, 89,
588 11749–11757, doi:10.1029/JD089iD07p11749, 1984.



589 Jouzel J., Merlivat L., Petit J. R., and Lorius C.: Climatic information over the last
590 century deduced from a detailed isotopic record in the South Pole snow, *Journal of
591 Geophysical Research*, 88, 2693–2703, doi:10.1029/JC088iC04p02693, 1983.

592 Jouzel J., et al.: Validity of the temperature reconstruction from water isotopes in ice
593 cores, *Journal of Geophysical Research*, 102, 26471–26487,
594 doi:10.1029/97JC01283, 1997.

595 Jouzel J., Vimeux F., Caillon N., Delaygue G., Hoffman G., Masson-Delmotte V., and
596 Parrenin F.: Magnitude of isotope/temperature scaling for interpretation of central
597 Antarctic ice cores, *Journal of Geophysical Research*, 108, 1–6,
598 doi:10.1029/2002JD002677, 2003.

599 Kaempfer T. U., and Schneebeli M. Observation of isothermal metamorphism of new
600 snow and interpretation as a sintering process, *Journal of Geophysical Research*,
601 112(D24), 1–10, doi:10.1029/2007JD009047, 2007.

602 Krinner G. and Werner M.: Impact of precipitation seasonality changes on isotopic
603 signals in polar ice cores: A multi-model analysis, *Earth and Planetary Science
604 Letters*, 216, 525–538, doi:10.1016/S0012-821X(03)00550-8, 2003.

605 Lorius C., Merlivat L., Jouzel J., and Pourchet M.: A 30,000-yr isotope climatic record
606 from Antarctica ice, *Nature*, 280, 644–648, doi:10.1038/280644a0, 1979.

607 Löwe H., Spiegel J. K., and Schneebeli M.: Interfacial and structural relaxations of
608 snow under isothermal conditions, *Journal of Glaciology*, 57, 499–510,
609 doi:10.3189/002214311796905569, 2011.

610 Masson-Delmotte V., Steen-Larsen H. C., Ortega P., Swingedouw D., Popp T., Vinther
611 B. M., Oerter H., Sveinbjornsdottir A. E., Gudlaugsdottir H., Box J. E., Falourd S.,
612 Fettweis X., Gallee H., Garnier E., Jouzel J., Landais A., Minster B., Paradis N.,
613 Orsi A., Risi C., Werner M., and White J. W. C.: Recent changes in north-west



614 Greenland climate documented by NEEM shallow ice core data and simulations,
615 and implications for past temperature reconstructions, *The Cryosphere*, 9, 1481-
616 1504, doi:10.5194/tc-9-1481-2015, 2015.

617 Merlivat L. and Jouzel J.: Global climatic interpretation of the deuterium-oxygen 18
618 relationship for precipitation, *Journal of Geophysical Research*, 84, 5029–5033,
619 doi:10.1029/JC084iC08p05029, 1979.

620 Neumann T. A.: Effects of firn ventilation on geochemistry of polar snow, PhD thesis,
621 University of Washington, Washington, USA, 2003.

622 Neumann T. A. and Waddington E. D.: Effects of firn ventilation on isotopic exchange,
623 *Journal of Glaciology*, 50, 183–194, 2004.

624 Neumann T. A., Albert M. R., Lomonaco R., Engel C., Courville Z., and Perron F.:
625 Experimental determination of snow sublimation rate and stable-isotopic exchange,
626 *Annals of Glaciology*, 49, 1–6, doi:10.3189/172756408787814825, 2008.

627 Otsu N.: A Threshold Selection Method from Gray-Level Histograms, *IEEE*
628 Transactions on Systems Man and Cybernetics, 9, 62–66, 1979.

629 Persson A., Langen P. L., Ditlevsen P., and Vinther B. M.: The influence of
630 precipitation weighting on interannual variability of stable water isotopes in
631 Greenland, *Journal of Geophysical Research – Atmosphere*, 116, 1-13,
632 doi:10.1029/2010JD015517, 2011.

633 Petit J. R., et al.: Climate and atmospheric history of the past 420,000 years from the
634 Vostok ice core, *Antarctica*, *Nature*, 399, 429–436, doi:10.1038/20859, 1999.

635 Pinzer B. R., Schneebeli M., and Kaempfer T. U.: Vapor flux and recrystallization
636 during dry snow metamorphism under a steady temperature gradient as observed by
637 time-lapse microtomography, *The Cryosphere*, 6, 1141–1155, doi:10.5194/tc-6-
638 1141-2012, 2012.



639 Ramseier R. O: Self-diffusion of tritium in natural and synthetic ice monocrystals,
640 Journal of Applied Physics, 38, 2553-2556, 1967.

641 Ritter F., Steen-Larsen H. C., Werner M., Masson-Delmotte V., Orsi A., Behrens M.,
642 Birnbaum G., Freitag J., Risi C., and Kipfstuhl S.: Isotopic exchange on the diurnal
643 scale between near-surface snow and lower atmospheric water vapor at Kohnen
644 station, East Antarctica, The Cryosphere Discussion, doi:10.5194/tc-2016-4, in
645 review, 2016.

646 Schleef S., Jaggi M., Löwe H., and Schneebeli M.: Instruments and Methods: An
647 improved machine to produce nature-identical snow in the laboratory, Journal of
648 Glaciology, 60, 94–102, 2014.

649 Sjolte J., Hoffmann G., Johnsen S. J., Vinther B. M., Masson-Delmotte V., and Sturm
650 C.: Modeling the water isotopes in Greenland precipitation 1959-2001 with the
651 meso-scale model remo-iso, Journal of Geophysical Research, 116, 1-22,
652 doi:10.1029/2010JD015287, 2011.

653 Steen-Larsen H. C., Masson-Delmotte V., Sjolte J., Johnsen S. J., Vinther B. M., Breon
654 F. M., Clausen H. B., Dahl-Jensen D., Falourd S., Fettweis X., Gallee H., Jouzel J.,
655 Kageyama M., Lerche H., Minster B., Picard G., Punge H. J., Risi C.,
656 Salas D., Schwander J., Steffen K., Sveinbjornsdottir A. E., Svensson A., and
657 White J.: Understanding the climatic signal in the water stable isotope records from
658 the neem shallow firn/ice cores in northwest Greenland, Journal of Geophysical
659 Research - Atmosphere, 116, 1–20, doi:10.1029/2010JD014311, 2011.

660 Steen-Larsen H. C., Johnsen S. J., Masson-Delmotte V., Stenni B., Risi C., Sodemann
661 H., Balslev-Clausen D., Blunier T., Dahl-Jensen D., Ellehøj M. D., Falourd S.,
662 Grindsted A., Gkinis V., Jouzel J., Popp T., Sheldon S., Simonsen S. B., Sjolte J.,
663 Steffensen J. P., Sperlich P., Sveinbjörnsdóttir A. E., Vinther B. M., and Whistle J.



664 W. C.: Continuous monitoring of summer surface water vapor isotopic composition
665 above the Greenland Ice Sheet, *Atmospheric Chemistry and Physics*, 13, 4815–
666 4828, doi: 10.5194/acp-13-4815-2013, 2013.

667 Steen-Larsen H. C., Masson-Delmotte V., Hirabayashi M., Winkler R., Satow K., Prié
668 F., Bayou N., Brun E., Cuffey K. M., Dahl-Jensen D., Dumont M., Guillevic M.,
669 Kipfstuhl S., Landais A., Popp T., Risi C., Steffen K., Stenni B., and
670 Sveinbjörnsdóttir A. E.: What controls the isotopic composition of Greenland
671 surface snow?, *Climate of the Past*, 10, 377–392, doi:10.5194/cp-10-377-2014.,
672 2014a.

673 Steen-Larsen H. C., Sveinbjörnsdóttir A. E., Peters A. J., Masson-Delmotte V.,
674 Guishard M. P., Hsiao G., Jouzel J., Noone D., Warren J. K., and White J. W. C.:
675 Climatic controls on water vapor deuterium excess in the marine boundary layer of
676 the North Atlantic based on 500 days of in situ, continuous measurements,
677 *Atmospheric Chemistry and Physics*, 14, 7741-7756, doi:10.5194/acp-14-7741-
678 2014., 2014b.

679 Sturm M. and Johnson J. B.: Natural convection in the subarctic snow cover, *Journal of*
680 *Geophysical Research*, 96, 11657–11671, doi:10.1029/91JB00895, 1991.

681 Town M. S., Warren S. G., Walden V. P., and Waddington E. D.: Effect of atmospheric
682 water vapor on modification of stable isotopes in near-surface snow on ice sheets,
683 *Journal of Geophysical Research-Atmosphere*, 113, 1-16,
684 doi:10.1029/2008JD009852, 2008.

685 Van der Wel G., Fischer H., Oerter H., Meyer H., and Meijer H. A. J.: Estimation and
686 calibration of the water isotope differential diffusion length in ice core records, *The*
687 *Cryosphere Discussion*, 9, 927-973, doi:10.5194/tc-9-1601-2015, 2015



688 Waddington E. D., Cunningham J., and Harder S. L.: The effects of snow ventilation on
689 chemical concentrations, in: Chemical Exchange Between the Atmosphere and
690 Polar Snow, edited by: Wolff, E. W. and Bales, R. C., Springer, Berlin, NATO ASI
691 Series, 43, 403–452, 1996.

692 Waddington E. D., Steig E. J., and Neumann T. A.: Using characteristic times to assess
693 whether stable isotopes in polar snow can be reversibly deposited. Annals of
694 Glaciology, 35, 118–124, doi:10.3189/172756402781817004, 2002.

695 Werner M., Langebroek P. M., Carlsen T., Herold M., and Lohmann G.: Stable water
696 isotopes in the ECHAM5 general circulation model: Toward high-resolution
697 isotope modeling on a global scale, Journal of Geophysical Research Atmosphere,
698 116, D15109, doi:10.1029/2011JD015681, 2011.

699 White J. W., Barlow L. K., Fisher D., Grootes P., Jouzel J., Johnsen S. J., Stuiver M.,
700 and Clausen H.: The climate signal in the stable isotopes of snow from Summit,
701 Greenland: Results of comparisons with modern climate observations, Journal of
702 Geophysical Research, 102, 26425–26439, doi:10.1029/97JC00162, 1997.

703 Zermatten E., Schneebeli M., Arakawa H., and Steinfeld A.: Tomography-based
704 determination of porosity, specific area and permeability of snow and comparison
705 with measurements, Cold Regions Science and Technology, 97, 33–40,
706 doi:10.1016/j.coldregions.2013.09.013, 2014.

707

708



709 **Table 1:** Morphological properties and flow characteristics of the experimental runs:

710 snow density (ρ), porosity (ε), specific surface area per unit mass (SSA), mean pore
711 space diameter (d_{mean}), superficial velocity in snow (u_D), corresponding Reynolds
712 number ($\text{Re} = d_{\text{mean}} \cdot u_D / v_{\text{air}}$), average inlet temperature of the humidifier and at the inlet
713 ($T_{\text{in,mean}}$), average outlet temperature at the outlet ($T_{\text{out,mean}}$), and average temperature
714 gradient (∇T_{ave}). Experiment (1) corresponds to the isothermal conditions; Experiment
715 (2) to air warming; and Experiment (3) to air cooling in the snow sample.

716

	ρ kg m ⁻³	ε –	SSA m ² kg ⁻¹	d_{mean} mm	u_D m s ⁻¹	Re –	$T_{\text{in,mean}}$ °C	$T_{\text{out,mean}}$ °C	∇T_{ave} K m ⁻¹
Experiment (1)	201.74	0.78	28.0	0.39	0.03	0.76	-15.5	-15.5	–
Experiment (2)	201.74	0.78	29.7	0.36	0.03	0.70	-15.4	-14.0	+47
Experiment (3)	220.08	0.76	27.2	0.37	0.031	0.74	-12.3	-14.1	-60

717



718 **Table 2:** $\delta^{18}\text{O}$ in the vapor in the humidifier ($\delta^{18}\text{O}_{\text{hum}}$) and of the snow in the sample
719 holder ($\delta^{18}\text{O}_s$) at the beginning ($t = 0$) and end ($t = \text{end}$) of each experiment and the final
720 $\delta^{18}\text{O}$ content of the snow in the sample holder at the inlet ($z = 0$ mm) and outlet ($z = 30$
721 mm). Experiment (1) corresponds to the isothermal conditions; Experiment (2) to air
722 warming; and Experiment (3) to air cooling in the snow sample.

723

	$\delta^{18}\text{O}_{\text{hum}}$		$\delta^{18}\text{O}_{s, t = 0}$		$\delta^{18}\text{O}_{s, t = \text{end}}$	
	‰		‰		‰	
	$t = 0$	$t = \text{end}$			$z = 0$ mm	$z = 30$ mm
Experiment (1)	-68.2	-67.5	-10.97	-17.75	-15.72	
Experiment (2)	-66.3	-66.1	-11.94	-19.60	-16.60	
Experiment (3)	-62.8	-62.2	-10.44	-25.53	-15.00	

724



725 **Figure captions**

726 **Fig. 1.** Schematic of the experimental setup. A thermocouple (TC) and a humidity
727 sensor (HS) inside the humidifier measured the the mean temperature and
728 humidity of the airflow. Two thermistors (NTC) close to the snow surface
729 measured the inlet and outlet temperature of the airflow (Ebner et al., 2014).

730 The Picarro Analyzer measured the isotopic composition $\delta^{18}\text{O}$ of the outlet
731 flow. Inset: 3D structure of $110 \times 42 \times 110$ voxels ($2 \times 0.75 \times 2 \text{ mm}^3$)
732 obtained by the μCT .

733 **Fig. 2.** Temporal isotopic composition of $\delta^{18}\text{O}$ of the outflow for each of the
734 experimental run. The spikes in the $\delta^{18}\text{O}$ were due to small temperature
735 changes in the cold laboratory (Ebner et al., 2014). Exp. (1) corresponds to
736 the isothermal conditions; Exp. (2) to air warming; and Exp. (3) to air
737 cooling in the snow sample. The higher the recrystallization rate of the snow
738 the slower the adaption of $\delta^{18}\text{O}$ of the outlet air to the inlet air. The
739 illustration in the lower right corner shows the relation between $\delta^{18}\text{O}$ of the
740 initial snow, inlet, and outlet of the air.

741 **Fig. 3.** Spatial isotopic composition of $\delta^{18}\text{O}$ of the snow sample at the beginning (t
742 = 0) and at the end (t = end) for each experiment. The air entered at $z = 0$
743 mm and exited at $z = 30$ mm. Exp. (1) corresponds to the isothermal
744 conditions; Exp. (2) to air warming; and Exp. (3) to air cooling in the snow
745 sample.

746 **Fig. 4.** Schematic of isotopic fractionation of vapor and ice during sublimation.
747 Water molecules sublimate rapidly from a flat ice surface in dry air and are
748 immediately removed. The different in relative mass of H_2^{16}O and H_2^{18}O led
749 to an isotopic fractionation of vapor and ice. The isotopic fractionation is a



750 brief transient effect, possibly lasting only a few minutes. Time t represents
751 the transition from diffusion-dominated behavior (with fractionation on
752 sublimation) to sublimation-dominated behavior (in which nearly all H_2^{18}O
753 atoms are forced to enter the vapor phase).

754

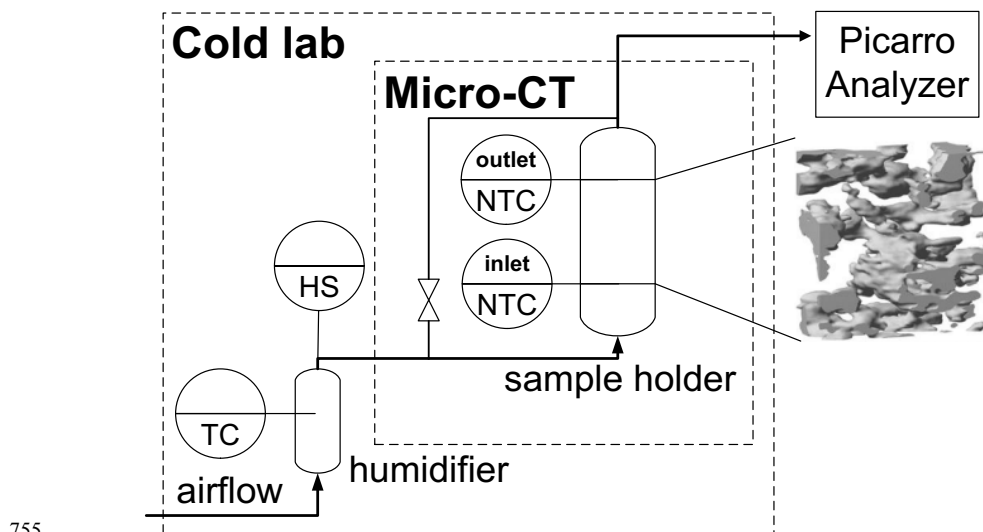
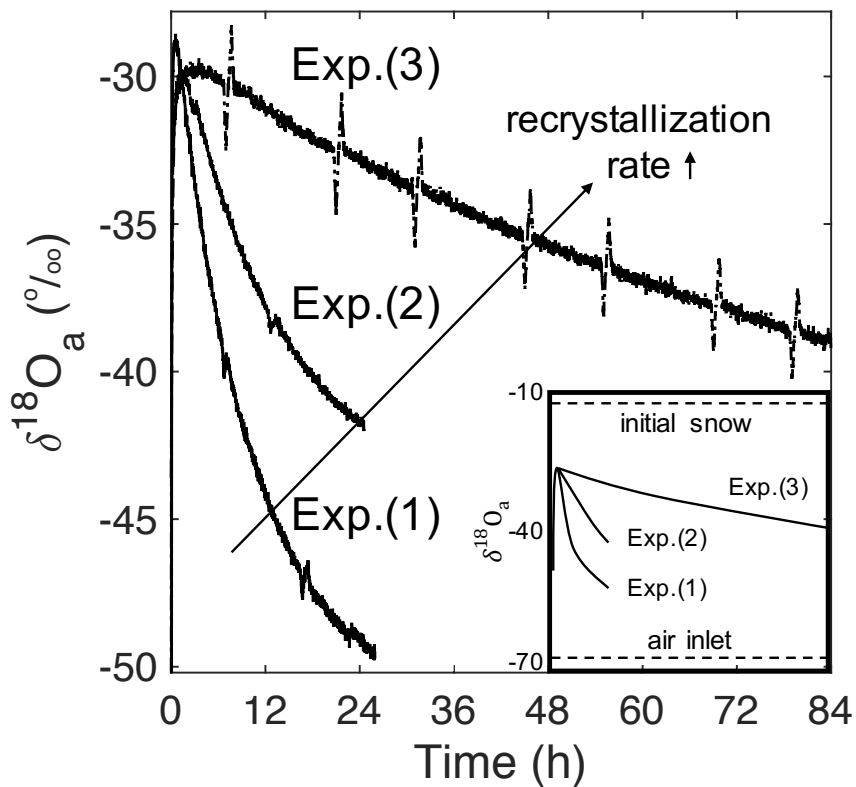


Fig. 1

755

756

757

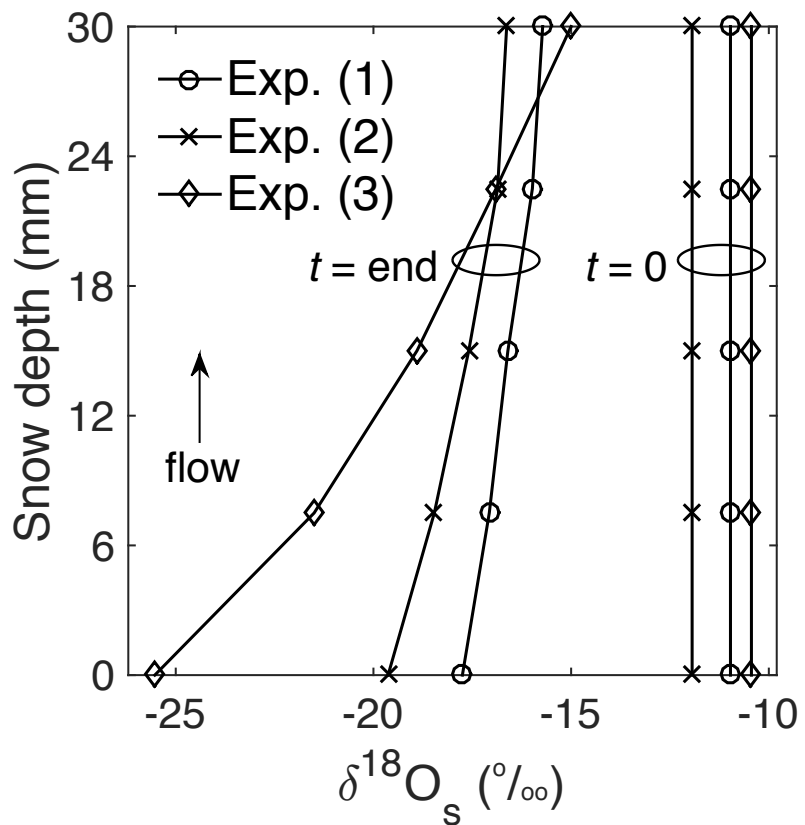


758

759

760

Fig. 2



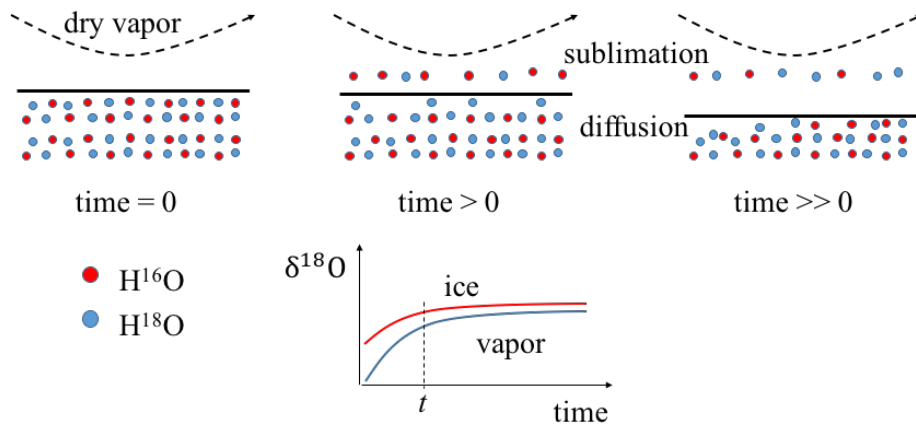
761

762

763

764

Fig. 3



765

766

Fig. 4